To be published in Optics Letters:

Title: Simultaneous measurement of displacement and temperature using balloon-like hybrid fiber sensor

Authors: João Santos,Joerg Bierlich,Jens Kobelke,Marta Ferreira

Accepted: 30 June 22

Posted 01 July 22

DOI: https://doi.org/10.1364/OL.465403

Simultaneous measurement of displacement and temperature using balloon-like hybrid fiber sensor

JOÃO P. SANTOS,[1] JÖRG BIERLICH,[2] JENS KOBELKE,[2] AND MARTA S. FERREIRA[1*]

[1]*i3N and Physics Department, University of Aveiro, Campus de Santiago, 3810-193 Aveiro, Portugal*
[2]*Leibniz Institute of Photonic Technology, Albert-Einstein-Straße 9, 07745 Jena, Germany*
**Corresponding author:* marta.ferreira@ua.pt

Received XX Month XXXX; revised XX Month, XXXX; accepted XX Month XXXX; posted XX Month XXXX (Doc. ID XXXXX); published XX Month XXXX

A fiber sensor based on a silica capillary in a balloon-like shape for simultaneous measurement of displacement and temperature is proposed and experimentally demonstrated. The sensor is fabricated by splicing a segment of a hollow core fiber between two single mode fibers (SMF) and by creating a balloon shape with the capillary at the top-center position. The SMF-capillary-SMF configuration excites an antiresonant (AR) guidance and the balloon shape enhances a Mach-Zehnder interferometer (MZI). Experimental results show that, for a balloon length of 4.0 cm and a capillary length of 1.2 cm, AR is insensitive to displacement and its sensitivity to temperature is 14.3 pm/°C, while the MZI has a sensitivity to displacement of 1.68 nm/mm, in a range between 0 and 5 mm, and of 28.6 pm/°C to temperature, twice the value of AR. The proposed fiber sensor has only one sensing element in one configuration which makes it of simple fabrication as well as low cost. © 2022 Optica Publishing Group

Sensors based on optical fibers have gathered great interest in a multitude of fields such as industrial or environmental monitoring, as well as health monitoring due to their compact size, high sensitivity, flexibility, and immunity to electromagnetic interference [1]. Measurement of displacement is of high demand for optical-based devices in applications where precise movement control is required such as aeronautics, microimaging, robotics and structural health monitoring [2-4]. The displacement fiber sensors usually adopt either a grating structure, such as Bragg gratings, long period and tilted gratings, or an interference-based principle, including multimode, Fabry-Perot, and Mach-Zehnder interferometers (MZI) [5-7]. Compared with interference-based fiber sensors, the grating-based ones require complex fabrication, involving precise phase masks, UV, CO_2 or femtosecond lasers, and a bulky optical setup for grating inscription, also increasing the associated cost [4].

As fiber sensors based on single mode fibers (SMFs) are bent, cladding modes are excited. This has led to the development of a balloon-like fiber sensor, which was first proposed by Y. Chen *et al.* under the name of droplet-like structure [8]. These balloons are made of stripped and bent SMF, which is fed through a tube placed so as to hold the balloon shape in position, maintaining its bending diameter.

To date, balloon-like sensors have only been developed with an SMF to form an MZI. To achieve simultaneous measurements, an optical element is usually cascaded: a fiber Bragg grating (FBG) [1], a long period grating (LPG) [6], or even a core-offset fiber [9], increasing the size of the sensor and its fabrication complexity. It has been demonstrated that these balloon-like interferometers possess high temperature cross-sensitivity and low displacement measuring range [10,11].

Therefore, it is desirable to develop a hybrid sensor for simultaneous measurement of high range displacement and temperature with only one sensing element.

In this Letter, a hybrid fiber sensor for simultaneous measurement of displacement and temperature based on a silica capillary tube spliced between two single mode fibers in a balloon-like structure is proposed. This configuration results in two interferometers occurring simultaneously in a single sensing element: antiresonant guidance (AR) and MZI.

The balloon-like fiber sensor is based on a SMF-capillary-SMF configuration. A segment of a hollow core silica capillary tube is spliced between two SMFs (Corning, SMF-28), as shown in **Fig**. 1a. The capillary has an inner diameter of 57 μm and an outer diameter of 125 μm, as seen in **Fig.** 1b. L, d, and n_1 are the capillary length, cladding thickness and SMF core RI, respectively. n_2 and n_0 are the refractive indices (RI) of the silica cladding and hollow core, 1.444 and 1.0 at 1550 nm [12], respectively.

For a certain capillary length above a certain critical value, due to a lower RI of the core compared to the cladding RI, an antiresonant reflecting optical waveguide (ARROW) occurs in which light is coupled into the cladding, forming an FP cavity defined by the M_1 and M_2 interfaces [14], as shown in **Fig.** 1a. The capillary used has a critical length of 300 μm. For a certain wavelength that meets the resonant condition of the cladding, the light escapes to the outside of the capillary, resulting in a low transmission intensity part of the transmission spectrum [15].

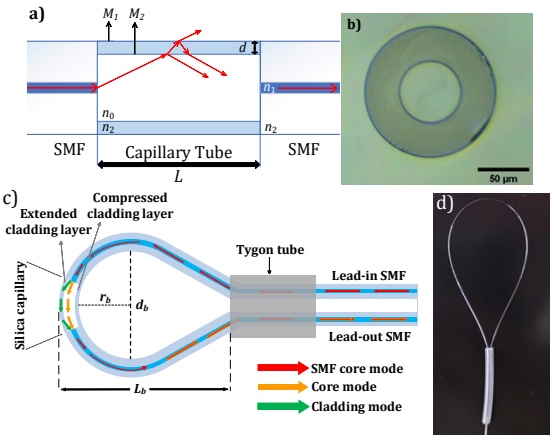

Fig. 1. (a) Antiresonant reflecting optical waveguide mechanism in the capillary. (b) Top view of the silica tube on a microscope. (c) Schematic diagram of the balloon-like sensor. (d) Picture of the fabricated sensor.

The balloon-like sensor has an arch shape where the silica capillary is placed at the top-center position of the balloon and the SMFs are fed through a capillary tube that is positioned accordingly (real photo shown in **Fig**. 1d). The length, bending diameter, and radius of the balloon are termed L_b, d_b, and r_b, respectively, as depicted in **Fig**. 1c.

When the light propagates through the lead-in SMF to the bending section, upon reaching the capillary instead of normally continuing its free path through its core, the bending of the fiber allows for a portion of the light to penetrate into the extended cladding, exciting the cladding mode, later coupling back to the core of the lead-out SMF. The difference in effective refractive index of the cladding and the core means that the optical path lengths are different, therefore creating an MZI.

The transmitted intensity of the balloon-like MZI can be expressed as [1]

$$I = I_{core} + I_{clad} + 2\sqrt{I_{core}I_{clad}}\cos(\Delta\phi), \quad (1)$$

where I_{core} and I_{clad} are the intensity of the core and cladding modes, respectively. $\Delta\phi$ is the phase difference between core and cladding modes, which is given by

$$\Delta\phi = \frac{2\pi(n_{core} - n_{clad})L}{\lambda} = \frac{2\pi\Delta nL}{\lambda}, \quad (2)$$

where λ is the wavelength of the light signal in free space, L is the length of the capillary length (not to be mistaken with the balloon length, L_b), n_{core} and n_{clad} are the effective RIs of the fundamental core mode and cladding mode, respectively, and Δn is the difference between the effective RIs. In this case, destructive interference will occur when the phase difference becomes an odd multiple of π, thus the dip wavelength can be expressed as

$$\lambda_m = \frac{2L * \Delta n}{2m + 1}, \quad (3)$$

where m is an integer. Its free spectral range (*FSR*) is given by

$$FSR_{MZI} = \frac{\lambda_{m+1}\lambda_m}{\Delta nL}. \quad (4)$$

As to the antiresonant guidance, the lossy dip occurs when it meets the resonant condition of the cladding, expressed as [13]

$$\lambda_m = \frac{2d}{m}\sqrt{n_2^2 - n_0^2}, \quad (5)$$

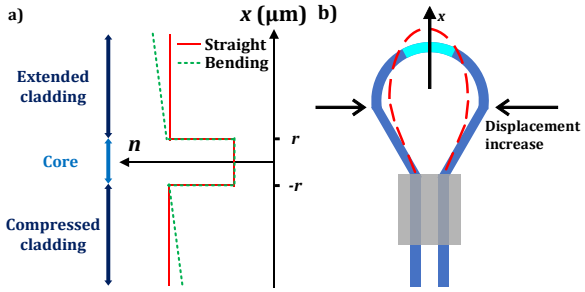

Fig. 2. (a) Refractive index profile of straight/bending fiber. (b) Schematic diagram of the balloon-like structure with displacement increase.

where m is the resonance order. Its *FSR* is given by

$$FSR_{AR} = \frac{\lambda_{m+1}\lambda_m}{2d\sqrt{n_2^2 - n_0^2}}. \quad (6)$$

As the balloon is bent, due to the elasto-optic effect, the RI increases in the extended layer of the bending fiber while for the compressed layer it diminishes. The refractive index model expressing the RI profile during bending is given by [1]

$$n'(x) = n(x)\left(1 + \frac{x}{r_b}\right), \quad (7)$$

where r_b is the bending radius, x is the perpendicular to the bending axis, $n'(x)$ and $n(x)$ are the RI profiles when the sensor is bent and straight, respectively.

When displacement is incrementally applied on the sensor, there is a decrease in the bending radius. Since the core is made of air, the RI will remain mostly the same during displacement increase, while the extended cladding layer will increase in effective RI and the compressed cladding layer will decrease in effective RI [1,5], as shown in **Fig.** 2a.

In this balloon configuration, the MZI only involves the cladding mode of the extended layer and the core mode [7]. According to (3), this increase in effective RI will lead to a shift in the transmission. For the AR guidance, this phenomenon occurs for both cladding layers of the capillary, meaning the increase in RI of the extended cladding will be compensated by the decrease in RI of the compressed cladding. Displacement does not affect the cladding thickness, therefore, according to (5), AR is expected to be insensitive to displacement in this balloon configuration.

The thermo-optic coefficient of silica is higher than that of air, so as temperature increases, the cladding mode RI will increase more than the RI of the core mode, increasing Δn. Moreover, due to the thermal expansion effect, an increase in temperature also results in the fiber expanding, increasing the value of L and d. According to the equations (3) and (5), this results in a positive shift in the transmission spectrum for both MZI and AR [16,17].

The transmission experimental setup, given in **Fig**. 3d, used for spectral analysis was comprised of a broadband light source (BBS) that emits on the C+L band with a wavelength range of 1530-1610 nm, and an optical spectrum analyzer (OSA, Anritsu, model MS9740A) with a 0.05 nm resolution.

The sensor was fabricated by fusion splicing in the manual mode of the Fujikura FMS-40S splicing machine with a power of 20 arb. un. and an arc time of 1500 ms without applying an offset. These parameters were chosen in a compromise between stronger splices that can withstand smaller bending diameters, without collapsing the sensor at the junction of the SMF and the capillary.

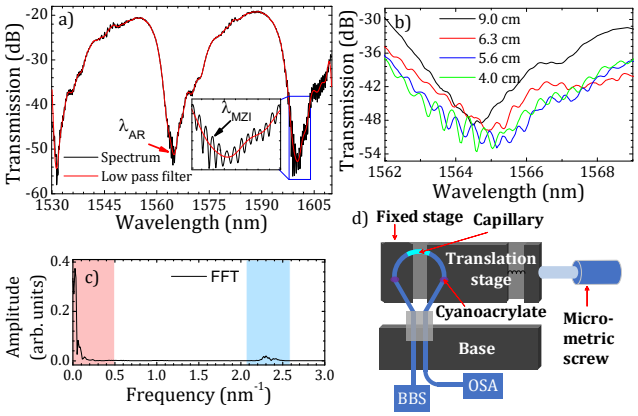

Fig. 3. Transmission spectrum for a 1.2 cm sensor with (a) 4.0 cm balloon length and (b) different balloon lengths. (c) FFT spectrum of the 4.0 cm balloon length sensor. (d) Schematic diagram of the displacement setup.

In order to achieve a balloon shaped fiber, the two ends of the SMFs were joined in a small segment of a Tygon® capillary tube that was moved upwards and adjusted until the fiber had an arch shape. Once the desired bending diameter was obtained, the fiber was glued on both tips of the Tygon® capillary tube with UV curable resin.

The transmission spectrum of a 1.2 cm long fiber sensor with no curvature, completely straight, reveals only well-defined periodic AR dips. In a balloon configuration with large length this result persists, however, as the balloon becomes smaller, the curvature on the capillary increases until a point where a low visibility, high frequency oscillation appears in the spectrum, corresponding to the MZI, as seen in **Fig**. 3b at 6.3 cm balloon length.

A smaller bending diameter results in more light penetrating into the cladding mode, resulting in an increase in the visibility of the MZI dips, as shown in **Fig.** 3b for balloon lengths of 5.6 and 5.2 cm. The increase of visibility is desired as it allows for an enhancement in resolution for sensing. However, if the bending diameter continues to decrease, an excess of light will penetrate into the cladding and even leak out of the fiber resulting in large attenuation [16].

For a 4.0 cm balloon length (bending diameter of 21.9 mm), the MZI is present throughout most of the spectrum. In order to obtain only the AR dips, a 0.5 nm^{-1} low pass filter was applied, as is depicted in **Fig**. 3a. The frequency of the filter was chosen based on this sensor's transmission spectrum FFT, as shown in **Fig**. 3c, where the AR region corresponds to the rectangle in pink. The MZI region is given by the blue rectangle.

In this sensor configuration, an MZI is present at up to 8.5 cm length balloons which is equivalent to a 45 mm bending diameter. This bending diameter is greater than the values presented by other works, with the highest found to be 14 mm [1].

Such a wide range of bending diameters manifesting MZI makes this sensor more versatile and durable, since smaller bending diameters can compromise the sensor due to higher tension applied on the fiber. Moreover, regardless of the bending diameter, AR guidance will always occur in transmission analysis.

When bent under stress the sensor was able to attain the smallest balloon length of 3 cm before breaking. Since the interferometers are enhanced for much longer balloon lengths, the probability of successful sensor preparation is, thus, assured for these lengths.

The capillary length was chosen as a compromise between the MZI visibility, AR visibility, and MZI enhancement. Capillary lengths shorter than 1 cm require smaller balloon bending diameters to enhance the MZI, possibly undermining the integrity of the sensor. Capillary lengths above 1.5 cm have less defined dips in the AR spectrum, making it more difficult to follow the dip during the characterizations.

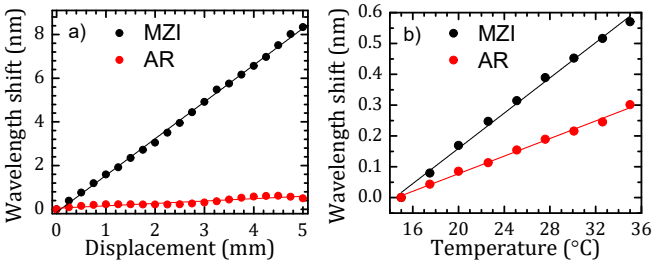

Fig. 4. Characterization of a balloon with 4.0 cm length and 1.2 cm capillary length to (a) displacement and (b) temperature.

For displacement measurement (setup shown in **Fig**. 3d) the balloon is placed between two translation stages and glued with cyanoacrylate at both sides, with the Tygon® tube laying on a base. One stage is fixed while the other is attached to a micrometer screw. Through the screw retraction, the platform moves horizontally, applying an incremental displacement on the balloon, which will become smaller in width and enlarge slightly in length, as shown in **Fig**. 2b.

The range of displacement applied was from 0 to 5 mm with steps of 0.25 mm. The dynamic range of these balloon-like sensors is around 20 mm, which is a wider range than previously reported [11]. The displacement response for both interferometers is given in **Fig.** 4a. The reference points where the wavelength shifts were measured for each interferometer are labeled in **Fig**. 3a.

The MZI shows a shift towards longer wavelengths (red shift), with a sensitivity of (1.68 ± 0.01) nm/mm, as well as high linearity (R^2 = 0.9986), while the AR component is practically insensitive to displacement with a value of (0.11 ± 0.01) nm/mm and an R^2 of 0.8646. This result is consistent with the theoretical analysis above.

For temperature characterization, the balloon was placed in a climate chamber (Weiss Technik) with controllable temperature and relative humidity, where the temperature was varied from 15 °C to 35 °C with steps of 2.5 °C and the relative humidity was kept constant at 60% RH.

The temperature response in **Fig**. 4b shows that both interferometers are sensitive to this parameter with a red shift. The MZI sensitivity is twice the AR sensitivity, of (28.6 ± 0.1) pm/°C for MZI versus (14.3 ± 0.1) pm/°C for AR. Both results have high linearity with R^2 = 0.9955 and R^2 = 0.9939 for MZI and AR, respectively. These values are comparable to previously obtained sensitivities in other works [13,17]. The temperature range is limited by the Tygon® tube high thermal expansion coefficient, which would compromise the sensor response for higher temperatures.

Due to the usage of UV glue, a temperature increase results in a change of volume and shape of the glue, interfering with the temperature results. Hitherto, this remains a limitation of this sensor. Replacing the Tygon® capillary with a silica capillary tube would grant great resistance to higher temperatures. Furthermore, the thermal expansion of the tube would no longer be an issue. On the other hand, glue would remain necessary, however a glue with higher temperature resistance could be utilized.

Since the sensitivities of the interferometers (MZI and AR) were different for both parameters, this sensor is a good candidate to

perform simultaneous measurement of displacement and temperature. A demodulation matrix can be established to calculate the changes of temperature (T) and displacement (D), which are given by

$$\begin{bmatrix}\Delta\lambda_{MZI}\\ \Delta\lambda_{AR}\end{bmatrix}=\begin{bmatrix}\kappa_{MZI}^{D} & \kappa_{MZI}^{T}\\ \kappa_{AR}^{D} & \kappa_{AR}^{T}\end{bmatrix}\begin{bmatrix}\Delta D\\ \Delta T\end{bmatrix} \quad (8)$$

where $\Delta\lambda$ is the wavelength shift (in nm) and κ is the sensitivity (in nm/°C or nm/mm). The variation of displacement and temperature can, thus, be expressed in the following matrix

$$\begin{bmatrix}\frac{\Delta D}{\Delta T}\end{bmatrix}=\frac{1}{0.020878}\begin{bmatrix}0.0143 & -0.0286\\ -0.11 & 1.68\end{bmatrix}\begin{bmatrix}\Delta\lambda_{MZI}\\ \Delta\lambda_{AR}\end{bmatrix} \quad (9)$$

Multiple sensors were developed, and coherent results were achieved in regards to its spectral and characterization results. Both the fabrication and characterization of the sensors showcased high repeatability. The stability of the sensor was assessed by continuously acquiring the sensor spectral response for 30 minutes. A standard deviation of 7 pm and 5 pm was achieved for MZI and AR, respectively, which is within the resolution limits of the OSA.

Table 1. Comparison of the sensing performance of different sensors for displacement and temperature measurement.

Sensing structure	Meas. Range (μm)	Disp. sens. (pm/μm)	Temp. sens. (pm/°C)	Ref.
Balloon + FBG[a]	0-70	180	105	[1]
2 core offset	0-1000	227	-	[4]
Balloon + LPG	0-80	-306	42.9	[6]
2 balloons	0-90	-318.8	47.4	[7]
Balloon + core-offset[a]	0-120	-528.57	-31.66	[9]
Balloon (MZI + ARROW)[a]	**0-5000**	**1.680**	**28.6 14.3**	**Our work**

[a]Hybrid sensors

From Table 1, it is clear the considerably higher displacement measuring range of the proposed sensor. Additionally, it is the only sensor to achieve simultaneous measurement in a hybrid configuration containing only one sensing element.

In conclusion, a fiber sensor based on silica capillary spliced between two SMFs in a balloon-like shape was proposed for the first time, to the best of our knowledge. The antiresonant guidance and MZI have different sensitivities to displacement and temperature, thus simultaneous measurement of these parameters can be achieved. The sensitivity of MZI to displacement and temperature was 1.68 nm/mm and 28.6 pm/°C, respectively. AR was insensitive to displacement and its sensitivity to temperature was of 14.3 pm/°C. The proposed fiber sensor has only one sensing element in one configuration which makes it of simple fabrication as well as low cost, with high measuring ranges of displacement.

Funding. This work was financially supported by the project AROMA, funded by FEDER, through CENTRO2020-Programa Operacional Regional do Centro, CENTRO-01-0145-FEDER-031568, and by national funds (OE), PTDC/EEI-EEE/31568/2017, UIDB/50025/2020 & UIDP/50025/2020, through FCT/MCTES. The work of Marta S. Ferreira was supported by the research fellowship CEECIND/00777/2018. The work was also funded by the German Federal Ministry of Education and Research (BMBF): "The Innovative Growth Core TOF" (Tailored Optical Fibers, FKZ 03WKCV03E) as well as the bilateral cooperation FCT/DAAD (FLOW, Project ID: 57518590).

Conflicts of Interest. The authors declare no conflict of interest.

Data Availability Statement. Data underlying the results presented in this paper are not publicly available at this time but may be obtained from the authors upon reasonable request.

References

1. Y. Wu, et al, "Simultaneous measurement of micro-displacement and temperature based on balloon-like interferometer and fiber Bragg grating," Optik, 183, 875-880 (2019).
2. X. Wen, et al, "High-sensitive microdisplacement sensor based on fiber Mach-Zehnder interferometer," IEEE Photonic Tech L, 26(23), 2395–2398 (2014).
3. J. Kokorian, et al, "In-plane displacement detection with picometer accuracy on a conventional microscope," J Microelectromech S, 24(3), 618–625 (2015).
4. J. Chen, J. Zhou and Z. Jia, "High-sensitivity displacement sensor based on a bent fiber Mach–Zehnder interferometer," IEEE Photonic Tech L, 25(23), 2354–2357 (2013).
5. X. Ding, T. Jin and R. Zhang, "Balloon-like angle and micro-displacement sensor based on bent single-mode fiber," Opt Fiber Technol, 68, 102787 (2022).
6. K. Tian, et al, "Simultaneous measurement of displacement and temperature based on balloon-shaped bent SMF structure incorporating an LPG," J Lightwave Technol, 1(1) (2018).
7. K. Tian, et al, "Simultaneous measurement of displacement and temperature based on two cascaded balloon-like bent fibre structures," Opt Fiber Technol, 58, 102277 (2020).
8. Y. Chen, et al, "Simultaneous measurement of refractive index and temperature using a cascaded FBG/droplet-like fiber structure," IEEE Sens J, 15(11), 6432-6436 (2015).
9. C. Li, et al, "A knotted shape core cladding optical fiber interferometer for simultaneous measurement of displacement and temperature," Photonic Nanostruct, 39, 100778 (2020).
10. X. Liu, et al, "High sensitivity balloon-like interferometer for refractive index and temperature measurement". IEEE Photonic Tech L, 28(13), 1485–1488 (2016).
11. L. Cai, X. Ai and Y. Zhao, "A displacement sensor based on balloon-like optical fiber structure," Sensor Actuat A-Phys 338, 113469 (2022).
12. I. H. Malitson, "Interspecimen comparison of the refractive index of fused silica," J. Opt. Soc. Am. 55, 1205-1208 (1965)
13. J. Zheng, et al, "An optical sensor designed from cascaded anti-resonant reflection waveguide and fiber ring-shaped structure for simultaneous measurement of refractive index and temperature," IEEE Photonic Tech L, 14(1) (2022).
14. X. Zhang, et al, "Transition of Fabry–Perot and antiresonant mechanisms via a SMF-capillary-SMF structure," Opt Lett, 43(10), 2268-2271 (2018).
15. R. Gao, et al, "Vibration sensor based on the resonance power leakage in a tapered capillary fiber," IEEE Sens J, 17(24), 8332–8337 (2017).
16. R. Tong, et al, "Simultaneous measurement of RH and temperature based on FBG and balloon-like sensing structure with inner embedded up-tapered MZI," Measurement, 146, 1-8 (2019).
17. B. Yue, et al, "Ultra-compact temperature sensor based on anti-resonant Mach-Zehnder interference," Opt Fiber Technol, 67, 102734 (2021).